SCIENCE OF LIGHT

VOLUME 8 NUMBER 1

July

1959

Published by the

Institute for Optical Research

Tokyo University of Education

in collaboration with

The Spectroscopical Society of Japan

SCIENCE OF LIGHT

Science of Light contains reports of the Institute for Optical Research and contribution from other science bodies about similar subjects.

All communications should be addressed to the director or to the librarian of the Institute.

The Institute for Optical Research

Tokyo University of Education

400, Hyakunin-tyo-4, Sinzyuku-ku, Tokyo, Japan

Printed at
the Printing Department, Chūō Kagakusha,
Tokyo

Effect of Gas Pressure on the Sensitivity of Pneumatic Cell

Kougo KAMIYA and Kunio YOSHIHARA

Department of Applied Physics, Faculty of Engineering, Nagoya University

(Received April 2, 1959)

Abstract

The sensitivity of pneumatic cell depends not only on its shape, but also on the nature and the pressure of used gas. This paper reports the results of calculation concerning the effect of gas pressure on the sensitivity of the cell. The optimum gas pressure is of the order of 10^{-1} atm. for both air and xenon cell, provided that the diameter and the depth of the cell are both 0.3 cm. The signal-to-noise ratio is, however, independent of gas pressure.

1. Introduction

One of the authors investigated the properties of pneumatic cell in detail on the basis of the theory of heat conduction[1], and pointed out that the usual pneumatic cell has maximum sensitivity at a pressure between 0.1 and 1 atm, but the numerical calculations were not carried out. In this paper the pressure dependence of the sensitivity will be discussed by carrying out actual calculations.

The displacement of the flexible mirror Δx, which represents the sensitivity of the cell is given approximately by[1]

$$\Delta x=\frac{1}{2}\varepsilon Q_0\frac{1}{2\kappa_r+2\kappa_g/d}\frac{1}{\sqrt{1+(2\pi\nu\tau)^2}}\frac{\mathrm{A}p}{T\left(\alpha+p\frac{A^2}{V}\right)} \tag{1}$$

This expression was derived originally for flat cells, but can be used for cylindrical cells as an approximation.

The following notations are used in the expression (1).

Q_0: the intensity of the incident radiation (cal/cm^2 sec.)
ε : the absorptive power of absorbing film.
κ_r : the cooling constant by radiation (cal/cm^2 sec. deg.)
κ_g : the heat conductivity of the gas (cal/cm sec. deg.)
d : half depth of the cell (cm)
ν : the chopping frequency. (cycles/sec.)
A : the area of the flexible mirror (cm^2)

1) K. Yoshihara: Science of Light, 7-3 (1958).

α : the constant of the restoring force of the flexible mirror (dynes/cm)

T : the absotute temperature of the ambient (deg.)

p : the internal gas pressure (dynes/cm^2)

V : the volnme of the cell (cm^3)

Time constant τ, which appears in the expression (1), is approximately given by

$$\tau=\frac{C_f+2dC_g\rho_g}{2\kappa_r+(\pi/2)^2(2\kappa_g/d)} \tag{2}$$

This was obtained also from the theory of heat conduction in the same way as the expression (1) was derived. Here, C_f is the heat capacity of the absorbing film per unit area (cal/deg. cm^2), C_g is the specific heat of the gas (cal/g. deg.) and ρ_g is the density of the gas (g/cm^3).

In the right side of the expression (1), $\frac{1}{2}\varepsilon Q_0(2\kappa_r+2\kappa_g/d)^{-1}\{1+(2\pi\nu\tau)^2\}^{-\frac{1}{2}}$ shows how the average temperature of the internal gas changes by the incident beam. Thus it is seen that the displacement of the mirror is obtained as the product of this factor and $Ap/T(\alpha+pA^2/V)$ which is derived from the equation of state for the gas.

2. Computation of Time Constant

Equation (2) for time constant was derived on the assumption that τ is almost equal to $C_f/2\kappa_r$. This assumption is nearly satisfied for the usual pneumatic cell.

The heat capacity C_f of the absorbing film is the sum of the heat capacities of the collodion film and the evaporated antimony. If the thickness of the collodion is 400 A, and that of the antimony is 200 A, the heat capacity of the former is 2.4×10^{-6} cal/deg. cm^2, and that of the latter is 6.65×10^{-7} cal/deg. cm^2,

Accordingly

$$C_f=3.06\times10^{-6}\ \text{cal/deg. cm}^2$$

As for d, we take the value corresponding approximatly to the maximum sensitivity at 1 atm. Then we have

$$d=0.2\ \text{cm for air and } d=0.1\ \text{cm for xenon}$$

$2\kappa_r$ is 1.47×10^{-4} cal/cm^2 sec. deg., $2\kappa_g$ is 1.13×10^{-4} cal/cm sec. deg. for air and 2.2×10^{-5} cal/cm sec. deg. for xenon as was shown in the previous paper. These values are independent of the gas pressure so far as the pressure is not too low.

On the other hand, reduction of gas pressure leads to the corresponding decrease of ρ_g and hence of $C_g\rho_g$. At 1 atm. the values of $C_g\rho_g$ for air and xenon are 2.90×10^{-4} cal/deg. cm. cm^3, and 2.22×10^{-4} cal/deg. cm.^{3} respectively.

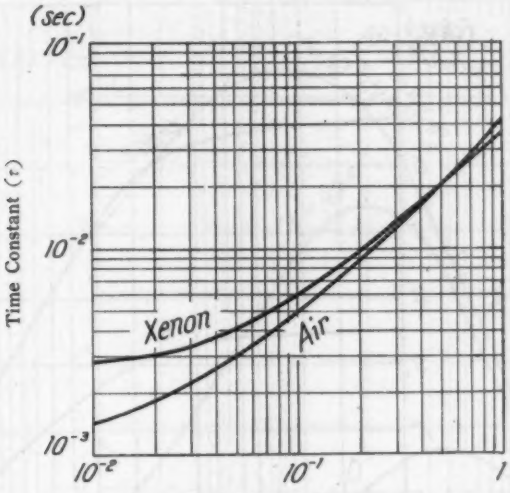

Fig. 1. Time Constant *vs.* Pressure Internal Gas.

In Fig. 1 is shown the variation of τ with gas pressure. As is seen from this figure, the time constant becomes shorter as the gas pressure is reduced.

3. Relation between the Sensitivity and the Gas Pressure

Now we estimate the sensitivity of the cell, using the time constant calculated in the previous section.

In equation (1), εQ_0 is the fraction of the incident radiation absorbed per unit area of absorbing film. ε is assumed to be 1/2. For convenience, we assume that Q_0 is 1 cal/cm^2 sec., though in reality Q_0 is very small. 10 cycles/sec. is assumed for ν.

First we calculate the average temperature variation ΔT_g caused by the incident radiation. We have for ΔT_g

$$\Delta T_g = \frac{1}{2}\varepsilon Q_0 \frac{1}{2\kappa_r + 2\kappa_g/d} \frac{1}{\sqrt{1+(2\pi\nu\tau)^2}} \tag{3}$$

Calculation of ΔT_g is carried out by substituting the numerical value of τ in this expression. The results are shown in Fig. 2.

As is shown in Fig. 2 ΔT_g increases at first rapidly with decrease of the gas pressure, but approaches gradually a constant value.

Next, by multiplying ΔT_g by the factor

$$Ap/T(\alpha + pA^2/V) \tag{4}$$

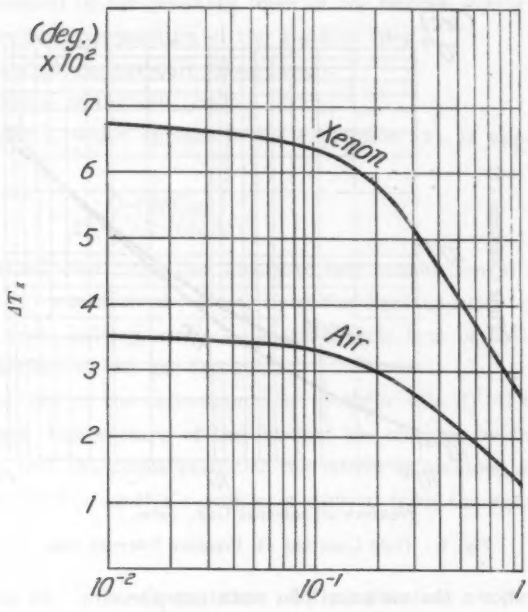

Fig. 2. Gas Temperature Increase for Unit Incidence *vs.* Internal Gas Pressure.

we obtain the sensitivity Δx. Here, A is 7×10^{-2} cm² and V is $2\pi a^2 d$, which is 2.38×10^{-2} cm³ for air cell and 1.42×10^{-2} cm³ for xenon cell. The constant of restoring force α of the flexible mirror is between 10^3 and 10^5 dynes/cm. Hence, Δx was calculated for the case when this force constant is 10^3, 10^4 and 10^5 dynes/cm respectively. The ambient temperature is assumed to be always 300°K. The sensitivity thus obtained is given in Fig. 3 for air and in Fig. 4 for xenon.

The pressure, at which the maximum sensitivity occurs, shifts towards higher pressure with increase of α, but the sensitivity itself falls down considerably. For usual value of α, the maximum sensitivity is nearly at 2×10^{-1} atm.

Lastly we estimate the sensitivity of the flat cell for which $a \gg d$. In this case V is very large and A^2/V is negligibly small. Hence we have

$$Ap/T(\alpha+A^2/V)=Ap/T\alpha$$

As is shown in Fig. 5, the sensitivity of such a cell has no maximum when p is smaller than 1 atm. It decreases monotonously with reduction of the gas pressure.

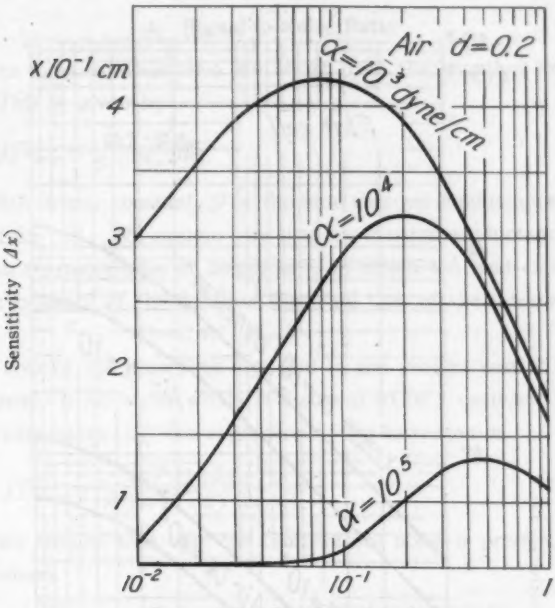

Fig. 3. Sensitivity of Cell *vs.* Internal Gas Pressure for Air

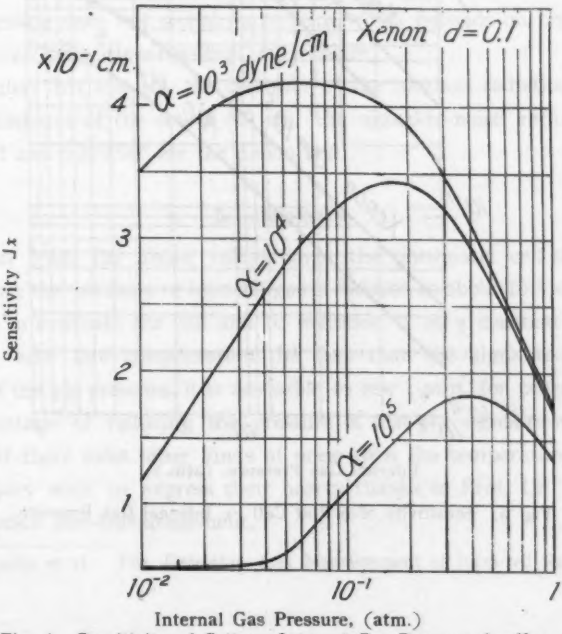

Fig. 4. Sensitivity of Cell *vs.* Internal Gas Pressure for Xenon.

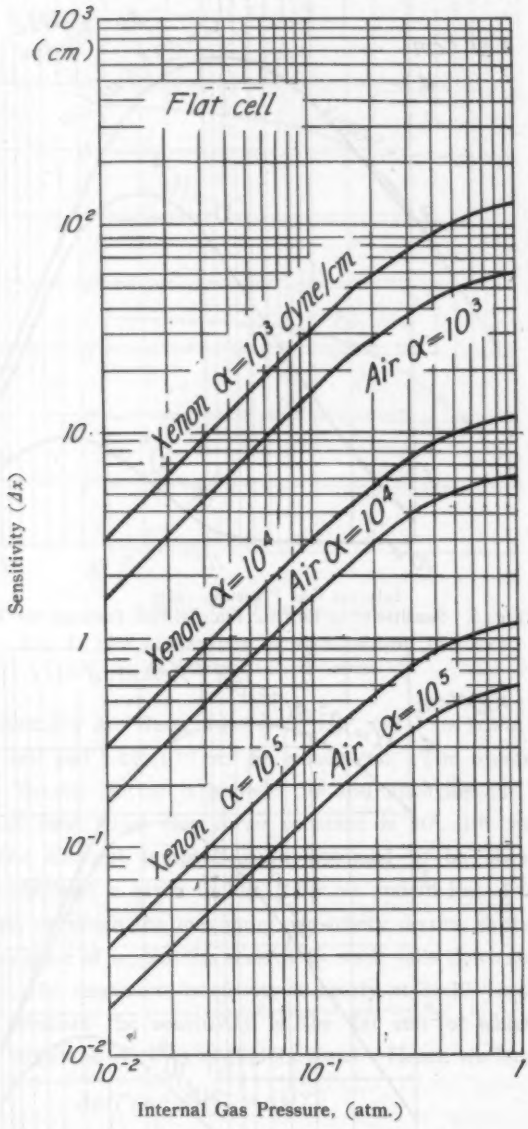

Fig. 5. Sensitivity of a Flat Cell *vs.* Internal Gas Pressure.

4. Signal-to-Noise Ratio

To obtain the signal-to-noise ratio, we strart from the equation for the thermal fluctuation[2]. This is given by

$$\overline{\Delta T^2}_{noise}=\frac{4kT^2\mathcal{G}\Delta\nu}{\mathcal{G}+(2\pi\nu C)^2} \tag{5}$$

where k is the Boltzmann constant, $\mathcal{G}$ is the total thermal conductance and $\mathcal{C}$ is the heat capacity of the cell. We assume here that the thermal conductance $\mathcal{G}$ is $\mathcal{C}/\tau$ as is the case with thermocouples or bolometers, in which the heat capacity $\mathcal{C}$ is the sum of the heat capacity of the collodion film and that of the internal gas, namely

$$\mathcal{C}=C_fA'+C_g\rho_gV$$

A' is the area of the absorbing film and in the present case it is equal to A. $\Delta\nu$ is the frequency band width which is assumed to be 1 cycle/sec.

Using the expression (2), the expression (5) is rewritten as

$$\overline{\Delta T^2}_{noise}=\frac{4kT^2\{1+2\pi\nu\tau)^2\}}{A\{2\kappa_r+(\pi/2)^2(2\kappa_g/d)\}} \tag{6}$$

Thus, if we assume that only the temperature noise is present, the signal-to-noise ratio becomes

$$\frac{\overline{\Delta T_g}}{\sqrt{\overline{\Delta T^2}_{noise}}}=\frac{\varepsilon Q_0}{2}\,\frac{1}{2\kappa_r+2\kappa_g/d}\,\frac{\sqrt{A\{2\kappa_r+(\pi/2)^2(2\kappa_g/d)\}}}{2T\sqrt{k}} \tag{7}$$

This expression does not contain any term which depends on pressure. Thus the signal-to-noise ratio is independent of pressure.

If we assume that ε is 1/2, the intensity of the incident radiation is 1 cal/sec. cm^2 and the diameter of the cell is 0.3 cm, the signal-to-noise ratio is 4.63×10^9 for the air cell and 5.31×10^9 for the xenon cell.

5. Summary

As is seen from the above calculations, the pneumatic cell shows the best sensitivity when the pressure of internal gas is reduced to about 10^{-1} atm. But, it is fairly difficult to evacuate the cell and to maintain it at a constant low pressure. Hence, if we take into consideration the fact that the signal-to-noise ratio is independent of the gas pressure, it is advisable to use 1 atm. for practical purposes.

The advantage of reducing the pressure is that the signal-to-noise ratio will be improved if there exist other kinds of noise than the temperature noise.

The authors wish to express their hearty thanks to Prof. Dr. Tarô Suga for his kind guidance and encouragement.

2) R.A. Smith et al.: The Detection and Measurement of Infra-red Radiation; (Oxford 1957) 206.

Properties of Pneumatic Infra-red Detector (II)

Kunio YOSHIHARA

Department of Applied Physics, Faculty of Engineering, Nagoya University.

(Received May 29, 1959)

Abstract

The response of the pneumatic cell to the periodical incident radiation is calculated by solving exactly the equation of heat conduction for the cell. The results are in good agreement with those of the previous paper which are obtained on the assumption that the cell can be regarded approximately as a detector with only one time constant.

Hence, it is ascertained that the calculations in the previous paper gives reliable data on the performance of the cell.

1. Introduction

In the previous paper[1], we used the following expression for the response of the pneumatic cell to the periodical incident radiation

$$(\overline{\Delta T_g})_\nu=(\overline{\Delta T_g})_0 \frac{1}{\sqrt{1+(2\pi\nu\tau)^2}} \qquad (1)$$

where $(\overline{\Delta T_g})_\nu$ is the amplitude of the mean temperature change of the gas in the cell, $(\overline{\Delta T_g})_\nu$ is the mean temperature rise of the gas for the constant incident radiation, ν is the chopping frequency and τ is the time constant. This expression is valid only when we can regard the cell as a detector with only one time constant. In reality, however, the cell has an infinite number of time constants as was shown in the previous paper and the expression (1) does not give the exact behaviour of the pneumatic cell.

In deriving (1), we assumed for simplicity that only the largest time constant is to be taken into account and the effects of others may be neglected. Although this assumption is presumably valid in usual cases, yet it is necessary to evaluate the exact response of the cell to the periodical incident radiation in order to ascertain the correctness of the expression (1).

2. Response of the Pneumatic Cell to the Periodical Incident Radiation

The schematic diagram of the cell is shown in Fig. 1 of the previous report.

1) K. Yoshihara: Science of Light, 7, (1958) 67

The pneumatic chamber is a cylindrical cavity with the diameter of $2a$ cm and the length of $2d$ cm. The origin of the co-ordinates is the center of the cylinder and the z-axis is the axis of the cylinder. The xy-plane coincides with the heat absorbing film.

Let the incident power be $(Q/\varepsilon)e^{-i\omega t}$, ε is the absorptive power of the absorbing film and ω represents $2\pi\nu$. Q is in general a function of r and θ. (we shall use hereafter the cylindrical co-ordinates) In reality the incident power is always positive and we must put it to be $(Q/\varepsilon)(1+e^{-i\omega t})$. But the results are the same as far as the amplitude of the temperature change is concerned.

Then the equations to be solved are

$$\frac{\partial(\Delta T_g)}{\partial t}=k\nabla^2(\Delta T_g) \tag{2}$$

$$\Delta T_g=0 \qquad \text{when } z=d \tag{3}$$

$$\Delta T_g=0 \qquad \text{when } r=a \tag{4}$$

$$\Delta T_g=\Delta T_f \qquad \text{when } z=0 \tag{5}$$

$$C_f\frac{\partial(\Delta T_f)}{\partial t}=Qe^{-i\omega t}+2\kappa_g\left(\frac{\partial(\Delta T_g)}{\partial z}\right)_{z=0}-2\kappa_r\,\Delta T_f \tag{6}$$

where the following notations are used;

ΔT_g=the difference between the gas temperature and the ambient temperature.

ΔT_f=the difference between the temperature of the heat absorbing film and the ambient temperature

$k=\kappa_g/\rho_g C_g$

κ_g=the heat conductivity of the gas in the cell.

ρ_g=the density of the gas.

C_g=the specific heat of the gas.

C_f=the heat capacity of the absorbing film per unit area.

κ_r=the radiation cooling constant.

Here we consider only the right half of the pneumatic chamber, hence we double both the radiation and conduction losses instead. The solution for ΔT_g is symmetrical with respect to the xy-plane. Though it is continuous at $z=0$, $\partial(\Delta T_g)/\partial z$ is not continuous there.

From physical considerations, ΔT_g is axially symmetric if Q is independent of θ. Then, putting $\Delta T_g=U(t)R(r)\Theta(\theta)Z(z)$ we have

$$\frac{1}{U}\frac{dU}{dt}=k\left(\frac{1}{R}\frac{d^2R}{dr^2}+\frac{1}{R}\frac{1}{r}\frac{dR}{dr}+\frac{1}{Z}\frac{d^2Z}{dz^2}\right)$$

Put this expression equal to $-i\omega$, and we have

$$\left.\begin{aligned} &U=e^{-i\omega t} && \text{(a)}\\ &\frac{1}{R}\frac{d^2R}{dr^2}+\frac{1}{R}\frac{1}{r}\frac{dR}{dr}+\frac{1}{Z}\frac{d^2Z}{dz^2}=-\frac{i\omega}{k} && \text{(b)}\end{aligned}\right\} \tag{7}$$

Put $(i\omega)/k=\alpha^2+\beta^2$, and we obtain

$$\frac{d^2R}{dr^2}+\frac{1}{r}\frac{dR}{dr}+\alpha^2R=0 \tag{8}$$

$$\frac{d^2Z}{dz^2}=-\beta^2Z \tag{9}$$

The particular solution of (8) is

$$R=J_0(\alpha r) \tag{10}$$

where from the condition (4)

$$J_0(\alpha a)=0$$

Thus αa is the root of the Bessel function. Hereafter we use μ_n $(n=1, 2, \cdots\cdots)$ instead of α.

The solution of (9) is

$$Z=c_1\cos\beta z+c_2\sin\beta z$$

where c_1 and c_2 are constants. According to the condition (3), Z becomes

$$Z=\sin\left\{\beta(d-z)\right\} \tag{11}$$

Since we have put $\alpha^2+\beta^2=\frac{i\omega}{k}$, we have

$$\beta^2=-\mu_n^2+\frac{i\omega}{k} \tag{12}$$

From (7a), (10) and (11), ΔT_g becomes

$$\Delta T_g=Ae^{-i\omega t}J_0(\mu_n r)\sin\beta(d-z) \tag{13}$$

where A is a constant which must be determined by the boundary condition.

Then, from the condition (5), we have

$$\Delta T_f=Ae^{-i\omega t}J_0(\mu_n r)\sin(\beta d) \tag{14}$$

Substituting (13) and (14) in (6) we obtain

$$\begin{aligned}&-i\omega C_f Ae^{-i\omega t}J_0(\mu_n r)\sin(\beta d)\\ &=Qe^{-i\omega t}-2\kappa_g A\beta e^{-i\omega t}J_0(\mu_n r)\cos(\beta d)-2\kappa_r Ae^{-i\omega t}J_0(\mu_n r)\sin(\beta d)\end{aligned} \tag{15}$$

For simplicity, assume that the distribution of the incident power is given by

$$Q=Q_0J_0(\mu_1 r) \tag{16}$$

where $\mu_1 r$ is the smallest root of J_0. Then, putting $\mu_n=\mu_1$, we have

$$A=\frac{Q_0}{2\kappa_g\beta\cos(\beta d)+2\kappa_r\sin(\beta d)-i\omega C_f\sin(\beta d)} \tag{17}$$

If the distribution of the incident power is not given by (16), the condition (6) cannot be satisfied unless the following more general expression is employed.

$$\Delta T_g=\sum A_n e^{-i\omega t} J_0(\mu_n r)\sin\{\beta_n(d-z)\}$$

Here, we do not consider such a general case.
Using (17), we have for ΔT_g

$$\Delta T_g=\frac{Q_0 e^{-i\omega t} J_0(\mu_1 r)\sin\{\beta(d-z)\}}{2(\kappa_r-i\omega c_f)\sin(\beta d)+2\kappa_g\beta\cos(\beta d)}$$

The average value of the temperature change of the gas is given by

$$\overline{\Delta T_g}=\int_0^d\int_0^{2\pi}\int_0^a \Delta T_g r\,dr\,d\theta\,dz/\pi a^2 d$$
$$=\frac{e^{-i\omega t}2J_1(\mu_1 a)Q_0\{1-\cos(\beta d)\}}{\mu_1 a\{\beta d(2\kappa_r-i\omega c_f)\sin(\beta d)+2\kappa_g\beta^2 d\cos(\beta d)\}} \tag{18}$$

The amplitude of the temperature change is $|\overline{\Delta T_g}|$. To get this value, we put

$$\beta=\xi+i\eta$$
$$1-\cos(\beta d)=A+iB$$
$$\beta d(2\kappa_r-i\omega c_f)\sin(\beta d)+2\kappa_g\beta^2 d\cos(\beta d)=C+iD$$

Then we have

$$\left.\begin{aligned}
A&=1-\cos(\xi d)\cosh(\eta d)\\
B&=\sin(\xi d)\sinh(\eta d)\\
C&=(2\kappa_r\xi+\omega C_f\eta)d\sin(\xi d)\cosh(\eta d)\\
&\quad+(-2\kappa_r\eta+\omega C_f\xi)d\cos(\xi d)\sinh(\eta d)\\
&\quad-2\kappa_g\mu^2_1 d\cos(\xi d)\cosh(\eta d)+\frac{2\kappa_g\omega d}{k}\sin(\xi d)\sinh(\eta d)\\
D&=(2\kappa_r\eta-\omega C_f\xi)d\sin(\xi d)\cosh(\eta d)\\
&\quad+(2\kappa_r\xi+\omega C_f\eta)d\cos(\xi d)\sinh(\eta d)\\
&\quad+\frac{2\kappa_g\omega d}{k}\cos(\xi d)\cosh(\eta d)+2\kappa_g\mu^2_1 d\sin(\xi d)\sinh(\eta d)
\end{aligned}\right\} \tag{19}$$

$$|\overline{\Delta T_g}|=\frac{2J_1(\mu_1 a)Q_0}{\mu_1 a}\sqrt{\frac{A^2+B^2}{C^2+D^2}}$$

For the flat cell where a is very large, μ_1 becomes very small because $\mu_1 a$ is a constant. If $\mu^2_1\ll\omega/k$, we have

$$\beta^2=\frac{i\omega}{k}$$

and hence

$$\beta=\pm\sqrt{\frac{\omega}{2k}}(1+i),\quad \xi=\eta+\sqrt{\frac{\omega}{2k}}$$

Then the expressions (19) become

$$\left.\begin{aligned}
A&=1-\cos(\xi d)\cosh(\xi d)\\
B&=\sin(\xi d)\sinh(\xi d)
\end{aligned}\right|$$

$$\left.\begin{aligned} C&=(2\kappa_r+\omega C_f)(\xi d)\sin(\xi d\omega)\cosh(\xi d)\\ &\quad+(-2\kappa_r+\omega C_f)(\xi d)\cos(\xi d)\sinh(\xi d)\\ &\quad+\frac{2\kappa_g\omega d}{k}\sin(\xi d)\sinh(\xi d)\\ D&=(2\kappa_r-\omega C_f)(\xi d)\sin(\xi d)\cosh(\xi d)\\ &\quad+2\kappa_r+\omega C_f)(\xi d)\cos(\xi d)\sinh(\xi d)\\ &\quad+\frac{2\kappa_g\omega d}{k}\cos(\xi d)\cosh(\xi d)\end{aligned}\right\}\quad(20)$$

To carry out the numerical calculation of $|\overline{\Delta T_g}|$, it is necessary to assign the dimensions of the cell, the physical constants appearing in the expressions above, etc.

We assume that they are all the same as those used in the previous paper. Thus we have in the case of the cell with finite diameter

$$\left.\begin{aligned}\xi&=22.8\,\mathrm{cm}^{-1}\\ \eta&=27.8\,\mathrm{cm}^{-1}\end{aligned}\right\}\ \text{for xenon cell}$$

$$\left.\begin{aligned}\xi&=8.80\,\mathrm{cm}^{-1}\\ \eta&=18.3\ \mathrm{cm}^{-1}\end{aligned}\right\}\ \text{for air cell}$$

when $a=0.15$ cm and $\nu=10$ c/s.

In the case of the flat cell, we have

$$\xi=\eta=25.2\,\mathrm{cm}^{-1}\ \text{for xenon cell}$$

$$\xi=\eta=12.7\,\mathrm{cm}^{-1}\ \text{for air cell}$$

when $\nu=10$ c/s.

The results of numerical calculations are shown in Figs. 1, 2, 3 and 4. These

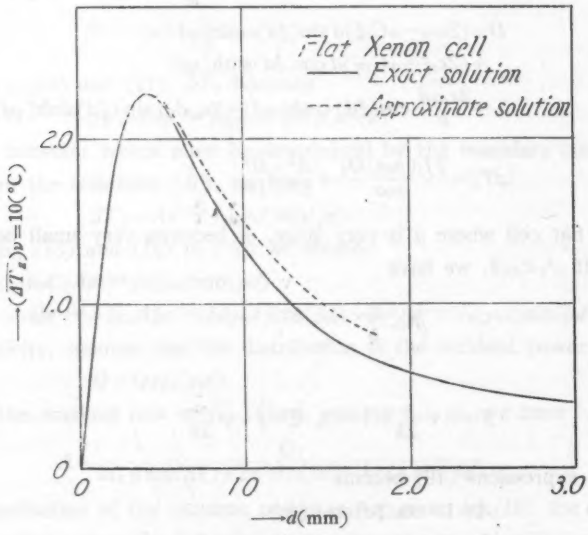

Fig. 1

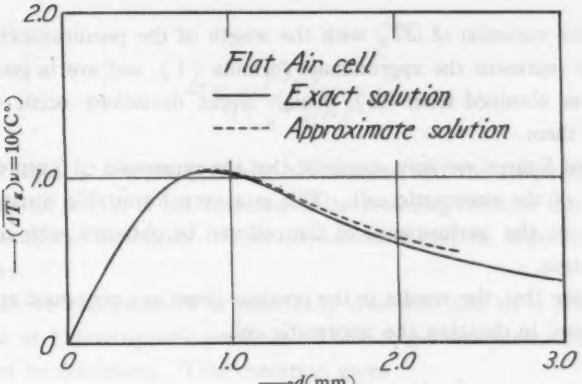

Fig. 2

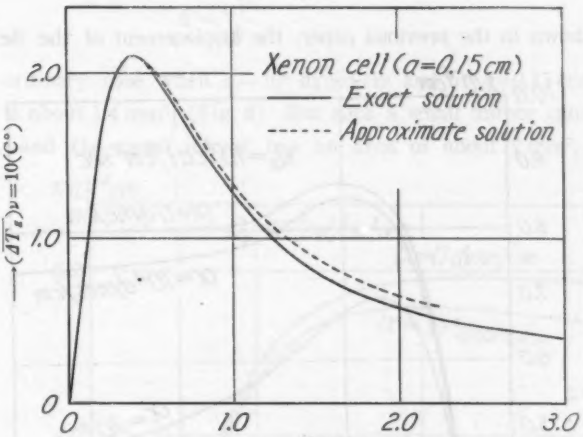

Fig. 3

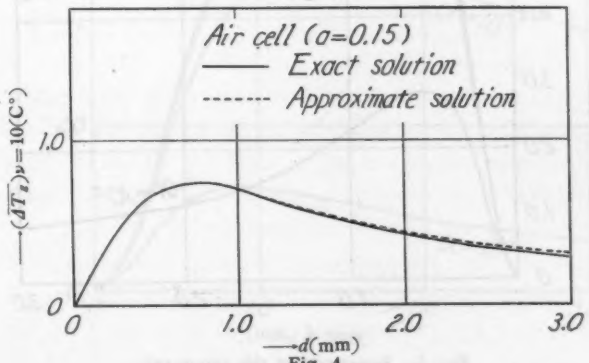

Fig. 4

figures give the variation of $|\overline{\Delta T_0}|$ with the length of the pneumatic chamber. The broken curves represent the approximate formula (1), and are in good agreement with the curves obtained from (21), though slight deviations occur towards the right ends of them.

From these figures we may conclude that the expression (1) represents closely the behaviour of the pneumatic cell. This is a very fovourable situation, because reliable data on the performance of the cell can be obtained with comparatively simple calculation.

Thus we see that the results in the previous paper are very good approximation and may be used in desiging the pneumatic cell.

3. Sensitivity of the Cell

As was shown in the previous paper, the displacement of the flexible mirror

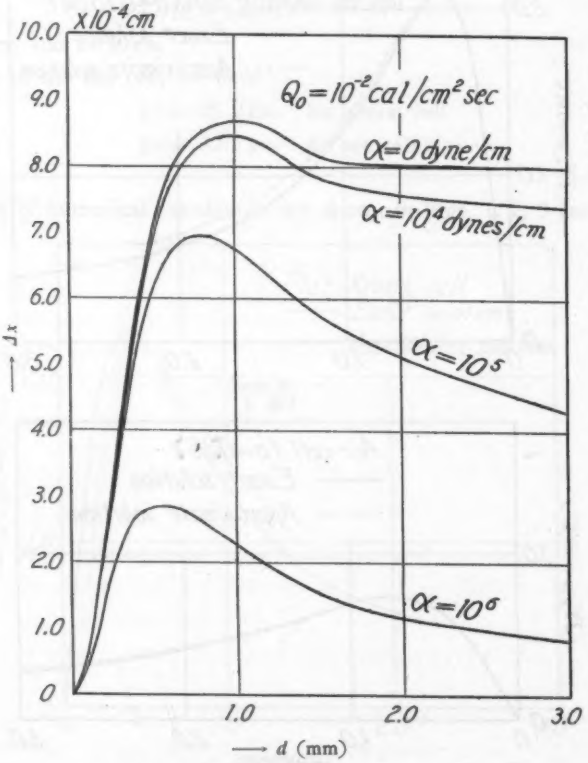

Fig. 5. Sensitivity of the xenon cell.

Δx is given by

$$\Delta x = \frac{p\overline{|\Delta T_\theta|}}{T\left(\frac{\alpha}{A}+\frac{p}{V}A\right)} \tag{21}$$

where p, V and T are the pressure, the volume and the temperature of the gas contained in the cell, α is the constant of the restoring force of the flexible mirror and A is the area of the mirror. This displacement may be regarded as a measure of sensitivity.

In the above expression T is practically constant, and so is p since the cell is usually kept at 1 atmospheric pressure. Thus, to get maximum sensitivity, $(\alpha/A+pA/V)$ must be minimum. This condition gives

$$A^2=\frac{\alpha V}{p} \tag{22}$$

In the ordinary case when $\alpha \approx 10^4$ dynes/cm and $a=d=0.15$ cm, the optimum value of A is about 1.4 mm². (Fig. 8) But such a small mirror cannot be realized in practice, and the usual mirror has an area of about 7 mm². Thus, in the

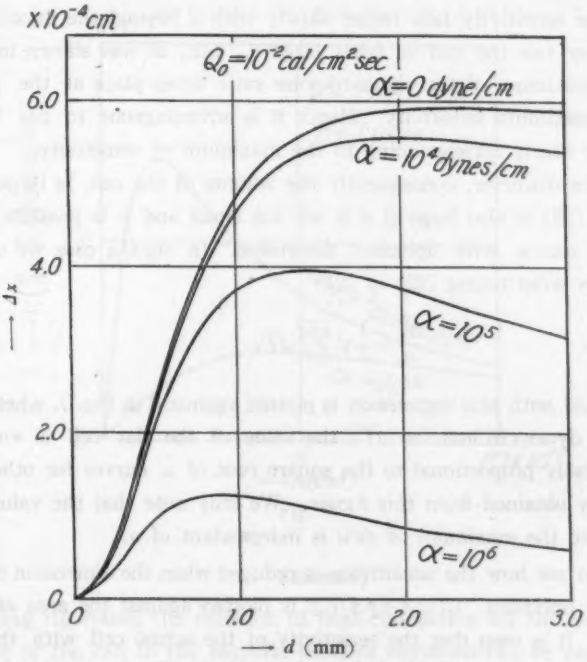

Fig. 6. Sensitivity of the air cell.

expression (21), A cannot take the optimum value but must take the practically possible value of 7 mm². Consequently, we may conclude that the sensitivity depends only on the restoring force and the length of the pneumatic chamber if the diameter of the chamber is fixed.

In Figs. 5 and 6 the sensitivity is plotted when α is 0, 10^4, 10^5 and 10^6 dynes/cm respectively. (a=0.15 cm)

These figures show that the sensitivity is almost independent of α if α is smaller than 10^4 dynes/cm, but when α exceeds 10^4 dynes/cm the sensitivity decreases remarkably with increase of α. Thus, on the one hand, the flexible mirror must not be too thick, but on the other, the use of extremely thin mirror is not advantageous because it is quite difficult to get an extremely thin mirror of good quality and that, in spite of this difficulty, the improvement of sensitivity is very small.

The optimum length of the pneumatic chamber at which the sensitivity has a maximum is somewhat smaller for xenon cell than for air cell, and this maximum shifts towards smaller value of d with increase of the resoring force. These facts are to be taken into account in actual construction of the cell.

Since the sensitivity falls rather slowly with d beyond the maximum, it seems that we may use the cell of fairly large d. But, as was shown in the previous paper, the maximum of the signal-to-noise ratio takes place at the point slightly left of the maximum sensitivity. Hence it is advantageous to use the cell with the length d nearly corresponding to the maximum of sensitivity.

When the diameter, consequently the volume of the cell, is large, the value of A given by (22) is also large if d is not too small and it is possible to construct the flexible mirror with optimum dimension. In such a case we obtain for the sensitivity by substituting (22) in (21)

$$\frac{\Delta x}{a}=\frac{1}{T}\sqrt{\frac{\pi pd}{2\alpha}}\,|\Delta T_0| \tag{23}$$

$\Delta x/a$ calculated with this expression is plotted against d in Fig. 7, where α is assumed to be 10^4 dynes/cm and for $|\Delta T_0|$ the value of the flat cell is employed. As $\Delta x/a$ is inversely proportional to the square root of α, curves for other value of α can be easily obtained from this figure. We may note that the value of d which corresponds to the maximum of $\Delta x/a$ is independent of α.

Lastly, to see how the sensitivity is reduced when the dimension of the flexible mirror is not optimum, $1/(\alpha/A+pA/V)$ is plotted against the area of the mirror A in Fig. 8. It is seen that the sensitivity of the actual cell with the mirror of 7 mm² falls to about one half of that of the ideal cell when $\alpha=10^4$ dynes/cm, but

when α exceeds about 10^3 dynes/cm, the selection of the area A is not critical.

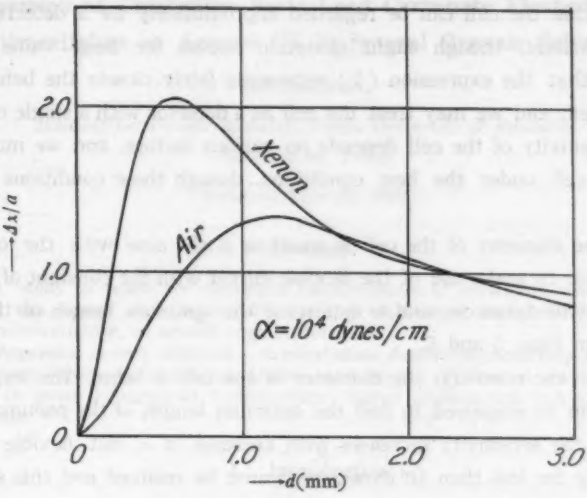

Fig. 7

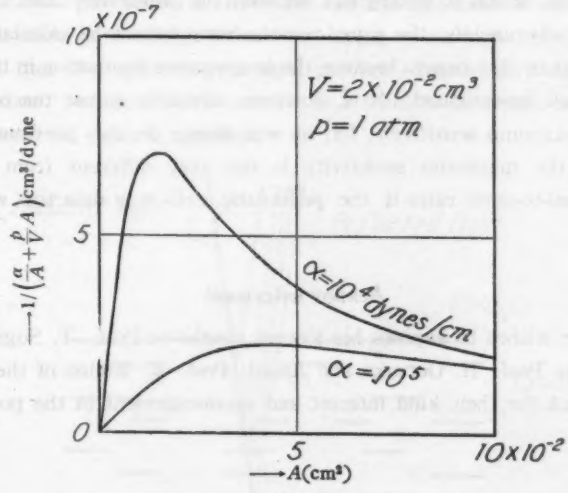

Fig. 8

4. Summary

By solving rigorously the equation of heat conduction for the pneumatic cell, the response of the cell to the periodic incident radiation can be calculated. The

results are in good agreement with those of the previous paper derived on the assumption that the cell can be regarded approximately as a detector with only one time constant, though slight deviation occurs for large value of d. This assures us that the expression (1) represents fairly closely the behaviour of the pneumatic cell, and we may treat the cell as a detector with a single time constant.

The sensitivity of the cell depends on various factors, and we must be careful to use the cell under the best conditions, though these conditions are not very critical.

When the diameter of the cell is small as is the case with the ordinary one, it is preferable to make use of the flexible mirror with the constant of the restoring force of about 10^4 dynes/cm, and to determine the optimum length of the pneumatic chamber from Figs. 5 and 6.

When, on the contrary, the diameter of the cell is large, the expression (23) or Fig. 7 is to be employed to find the optimum length of the pneumatic chamber. In this case, the sensitivity increases with decrease of α, but flexible mirrors for which α is by far less than 10^4 dynes/cm cannot be realized and this situation sets the practical limit of the sensitivity.

We must be careful to distinguish between the sensitivity and the signal-to-noise ratio. Unfortunately, the signal-to-noise ratio cannot be calculated from the results obtained in this paper, because the temperature fluctuation in the pneumatic cell is not well investigated. It is, however, advisable to use the cell under the condition of maximum sensitivity, for, as was shown in the previous paper, the condition for the maximum sensitivity is not very different from that for the maximum signal-to-noise ratio if the pneumatic cell is a detector with a single time constant.

Acknowledgement

The author wishes to express his sincere thanks to Prof. T. Suga for his kind guidance and to Prof. H. Ootsuka and Assist. Prof. K. Kudoo of the Institue for Optical Research for their kind interest and encouragement in the present work.

Dispersion of Crystalline Basic Lead Carbonate Flushed with Nitrocellulose or Aerosol OT in Several Organic Solvents

Sei HACHISU

Institute for Optical Research, Tokyo University of Education
Sinzyuku-ku, Tokyo

(Received June 22, 1959)

Abstract

A study is made on dispersive characteristics of crystalline white lead, which was treated with aerosol OT (sodium sulfonated dioctylsuccinate) or with nitrocellulose, in several organic solvents.

Dispersion is very selective. Nitrocellulose flushed pigment disperses only in solvents which dissolve nitrocellulose, and aerosol OT flushed one disperses only in polar halogenated hydrocarbons, higher alcohols and in a few other solvents.

1. Introduction

Basic lead carbonate deposits under proper conditions as very thin hexagonal platelet crystals of the radius of $10\mu \sim 20\mu$ and the thickness of 400Å~800Å.

These crystals have a high reflectivity owing to its high refractive index and are so thin that the scattering of light at their edges is very slight. They give out pearly sheen[1] when oriented parallel in a transparent media as shown in Fig. 1, and are used as a pearly pigment.

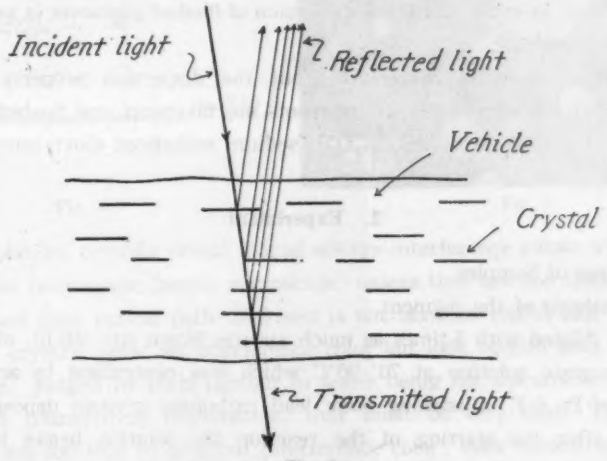

Fig. 1

1) Sei Hachisu: Science of Light, 6, No. 1, (1957) 20.

In using this pigment, it must be suspended in organic liquid vehicle. This processing is a rather difficult but important problem, for the constituent platelet crystals are very susceptible to coagulation and the coagulation damages fatally the characteristic pearly sheen of the pigment.

In ordinary pigments, the constituent particles are relatively globular; they contact each other only at very small area. Agglomeration of the particles are, therefore, weak and easily re-separable by kneading or working in a viscous vehicle. The agglomerates left to some extent in the pigment suspension do not cause so severe a hazzard as in the pearly pigment. The pigments are dried and ground into vehicles, or transferred directly into oily media which is called the "flushing" process. On the other hand, in the pearly pigment the particles are very thin platelets and the area of contact is so large in comparison with their volume that the agglomeration is very tight and not re-separable by kneading or working, and by hard kneading or working the platelets are crashed into white powder thoroughly losing the pearly sheen. It is apparent, therefore, that the pearly pigment should never be dried and ground but be transferred into oily media by flushing. Even in flushing, the platelets are liable to agglomerate and the technique of suspending the pearly pigment in a oily vehicle becomes a problem of great importance. In practice, it is flushed with nitrocellulose lacquer or with a solution of anionic surface active agents, and this flushed pigment in concentrated pasty form is formulated in any desired vehicle. But these flushed pigments are not always dispersible in every sort of vehicles but only in some particular kinds, in other words the dispersion of flushed pigments is very selective to the kinds of vehicle.

The present study is concerned about the dispersion property of flushed pigments. Two samples of flushed pigments are taken up, one flushed with nitrocellulose and the other with aerosol OT (sodium sulfonated dioctylsuccinate).

2. Experiment

1. Preparation of Samples.

(a) Synthesis of the pigment.

CO_2 gas diluted with 5-times as much air was blown into 500 lit. of 0.01 mol/l. basic lead acetate solution at 70°-90°C which was neutralised by acetic acid to the acidity of PH 6-7. Glistening basic lead carbonate crystals deposited and in 20-30 min. after the starting of the reaction the solution began to give out beautiful shiny stream lines. PH of solution decreased with the advance of reaction because of the yield of acetic acid from lead acetate, and concentrated solution

of basic lead acetate was added continuously throughout the reaction in order to maintain PH constant.

300-400 g of crystals were obtained in one batch. The suspension of crystals was concentrated by decantation. A thick liquid of silvery brilliance with the specific weight of 1.3-1.4 was obtained. It contained about 30% of basic lead carbonate crystals.

(b) The properties of the crystals (in mother liquid).

The chemical composition of the crystals was determined to be $2PbCO_3 \cdot Pb(OH)_2$ by gravimetric analysis of Pb and gas analysis of CO_2.

This crystal is optically uniaxial and negative; main refractive indexes are $\eta_\omega = 2.09$, $\eta_\varepsilon = 1.94$. A diagrammatical figure of the crystal is shown in Fig. 2. Fig. 3 is a microphotograph of this suspension, all the crystals existing separately.

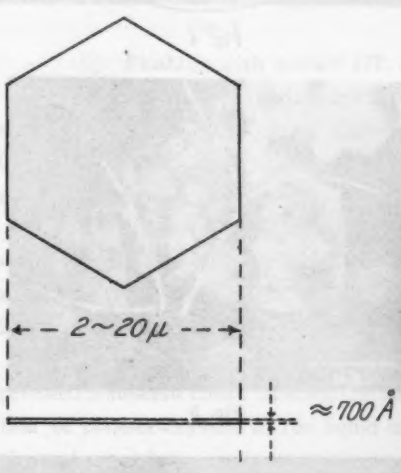

Fig. 2

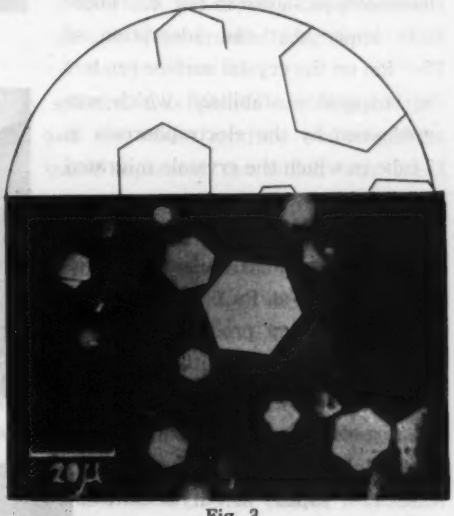

Fig. 3

Thin platelet crystals reveal almost always interference colors when observed by reflection microscope (metal microscope) unless they are too thick or too thin, namely when their optical path thickness is not between 1600 Å and 10,000 Å.

These crystals show no interference color but look blueish gray under metal-microscope. Judged by their contour in water being not discernible under microscope with transmitting illumination, they must be very thin. These crystals, therefore, are too thin to give out interference color; their optical path thickness is presumed to be less than 1,500 A. Refractive index is nearly 2, so the real thickness is expected to be less than 800 A[1].

This suspension of crystals is of a hydrophobic dispersion, hence it is rather unstable and susceptible to coagulation by the change of state of the mother liquid. When diluted with pure water to 50 times, the crystals begin to coagulate as shown in Fig. 4. The coagulation advanced on further dilution (100 times) as shown in Fig. 5 in which the agglomerates are marked by white border lines. When diluted with methanol, the crystals coagulated thoroughly as shown in Fig. 6. These facts imply that the adsorption of Pb^{++} ion on the crystal surface renders the suspension stabilized which was ascertained by the electrophoresis in U-tube in which the crystals migrated to cathode.

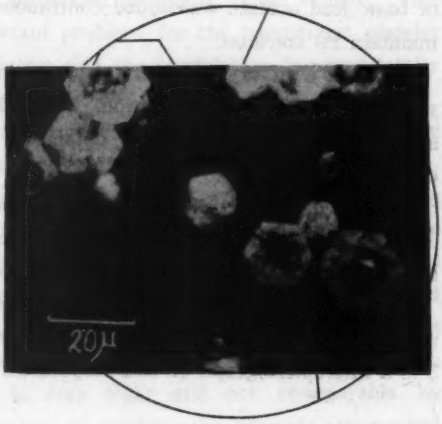

Fig. 4

The concentration of basic lead acetate for stabilized suspension was 0.05–0.01 mol/l at PH 6–7.

(c) Flushing process.

i) Flushing with nitrocellulose.

10 g of 15% solution of 1/2 sec. nitrocellulose (product of Asahi Kasei Ltd. Japan) in butylacetate was put into a small beaker, 30 g of the thick liquid of crystal suspension was added to it and the whole mixture was kneaded thoroughly. The crystals passed into the lacquer, and water that separated out as well-defined layer was poured off.

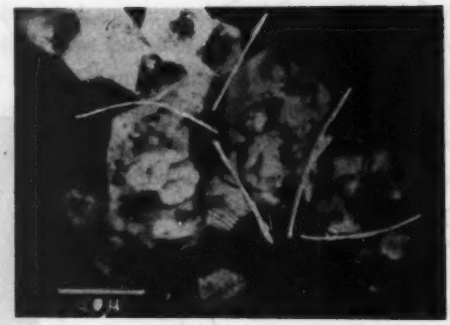

Fig. 5

Methanol was poured on the lacquer that had taken in the

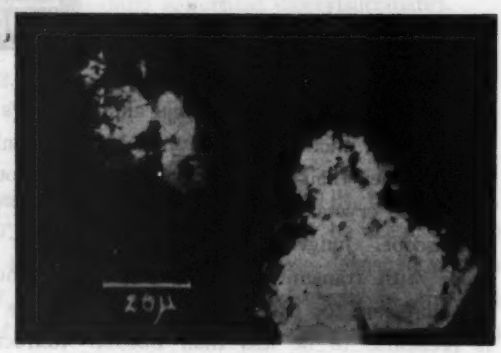

Fig. 6

crystals and the whole mixture was worked well. Water contained in the paste was extracted by methanol and the paste recovered the silvery sheen characteristic of the pigment. In order to remove excess nitrocellulose the paist was dissolved in ten-times as much solvent (butylacetate), centrifuged, and the supernatant liquid was removed. Further, the sediment was washed twice by decantation with ten times as much solvent. The final sediment was thinned by butylacetate to 60% of crystal content in weight. Microscopical feature was as shown in Fig. 7 in which the crystals dispersed well despite some crashed fragments.

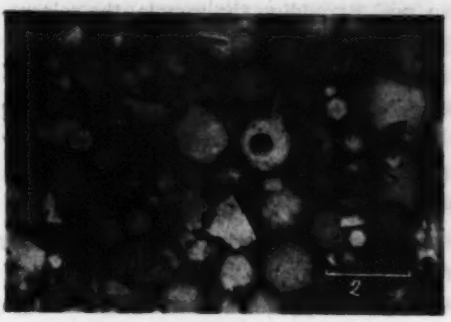

Fig. 7

ii) Flushing with aerosol OT.

10 cc of 5% aerosol in dichloromethane solution was poured on 80 g of the above-described thick aqueous suspension and the whole mixture was kneaded. Crystals passed into the organic phase and water separated out which was then poured off.

Organic phase turned into a soft paste, and excess aerosol was removed by washing the paste with fresh and well dehydrated dichloromethane in the same way as in i). Final suspension contained 60% of pigment and 40% of dichloromethane.

2. Properties of Samples.

These samples gave out bright silvery sheen, and moreover, almost always revealed iridescent colors on standing still. This is ascribed to the parallel orientation of platelet crystals in the liquid owing to the mutual repulsion of electrically charged crystals.

Zocher[2] studied this phenomenon in hydrosol of WO_3 and named it Schillar layer. It is interesting that this Schillar layer[2] can be formed also in organic phase. This shows that the repulsion force between particles reaches several thousand Å away, many times of the thickness of particles. These colored layers are observed in the case of pearl essence[3] consisting of guanine crystals collected from fish bodies.

The phenomenon of Schillar layer may be common to suspensions of platelet particles in general.

---

2) H. Zocher & K. Jacobsohn; Kolloid Beih. 28, (1929) 167.

3) D. Tressler, Marine Products of Commerce (1923); The Chemical Catalog Co. Inc. New York.

3. Selective dispersion of flushed crystals in several organic liquids.

A single drop of the sample was put from a glass rod of 3 mm in diameter into 5 cc of a solvent with which the dispersion of crystals was to be examined, and the mixture was thoroughly shaken up. By adding the sample, the solvent was obviously contaminated with butylacetate or dichloromethane which were initially present in the samples, but the comtaminating quantity was less than 0.5% in weight, and influence of them was negligible. By the time the dispersion was complete, the mixture gave out smooth pearly luster, which was however weakened when coagulation occurred. Between complete dispersion and thorough coagulation there were several steps. Four typical steps were picked up.

○···complete dispersion: mixture showed smooth pearly sheen, microscopic features are shown in Figs. 3 and 7.

△···slight coagulation: three or four crystals agglomerated as shown in Fig.

Table 1

Solvents		ε	Nitrocell. Flushed Pigment	Aerosol OT Flushed Pigment
Hydrocarbons	hexane	1.89	×	×
	xylene	2.77	×	×
	benzene		×	×
Esters	butylacetate	5.01	○	△
	ethylacetate	6.02	○	△
	linseed oil	3.35	×	×
	D.B.P.	6.43	○	×
Ketones	acetone	20.7	○	△
	M.E.K.	18.4	○	△
	M.B.K.	12.4	○	△
Alcohols	oleil alcohol		×	○
	butanol	17.1	×	○
	m-cresol	11.8	×	○
	cyxlohexanol	15.0	×	○
	ethanol	24.3	○	△
	methanol	33	○	×
Chloronated hydrocarbons	carbon tetrachloride	2.24	×	×
	monochlorobenzene	5.53	△	□
	o-dichlorobenzene	9.93	×	□
	dichloromethane	9.08	×	○
	chloroform	4.81	△	○
Others	ethyl ether		△	△
	ether+ethanol			
	pyridine	12.3	○	○
	nitromethane	35.9	○	○
	nitrobenzene	34.8	○	□
	ethylenglycol monomethyl ester		○	△
	diacetonealcohol		○	△
	furfural	41.9	○	○

ε: electric susceptibility

5, agglomerates sedimented fast, and in a few minutes, the supernatant liquid became clear in the case of non-viscous liquid. Pearly luster was not smooth.

×···strong coagulation: agglomeration was large enough to be recognized by the naked eye; no pearly luster; microscopical feature is shown in Fig. 6.

□···partial dispersion: suspension consists of dispersed crystals and coagulated ones as shown in Fig. 4; agglomerates sedimented fast, while dispersed part suspended stably and showed the pearly sheen.

The results are shown in Table 1. Remarkable trends are as follows.

a) Pigment flushed with nitrocellulose disperses only in liquids which dissolve nitrocellulose; it does not disperse in liquids which do not dissolve it.

b) Pigment flushed with aerosol disperses only in higher and aromatic alcohols, polar halogenated hydrocarbons and a few others but not in lower alcohols, in ketones and esters. Most liquids of good dispersion have fairly large values of electric susseptibility (ε are from 10-20), but in acetone, methanol and ethanol which have large value of ε, the dispersion is not good.

4. Discussion

Dispersive character of the crystals flushed with nitrocellulose may be explained as the effect of protective colloid action of nitrocellulose. On the other hand, the crystals flushed with aerosol OT have strange dispersion property. In general, particle surface treated with surface active agents becomes hydrophobic and oleophilic and the particles are expected to be dispersible in any sort of organic liquids, namely the crystals must be dispersible even in xylen, butylacetate and some other solvents. In spite of this expectation, the dispersion is very selective. This seems to be attributed to the extinction of adsorbed layer of aerosol-OT through dissolving into such liguids. But this is not the case because of the following facts.

1) After the separation of caogulated crystals from liquid by decantation, addition of dichloromethane causes re-dispersion of the coagulated crystals. If the coagulation were caused by the stripping off of adsorbed layer, this re-dispession would not occur.

2) Even if water is added to the liquid containing coagulated crystals and whole mixture is shaken up, the coagulated crystals do not pass into aqueous phase. This means that the surface of coagulating crystals is not hydrophic but oleophilic.

It is thus inferable that oleophilic particles do not always disperse in every sort of organic liquids. This property is seen also in other surface active agents such as sodium sulfonated alkylbenzene or oleic acid.

Dispersion and Electric Charge on Crystalline Basic Lead Carbonate—Treated with Nitrocellulose or Aerosol OT —in Several Organic Solvents.

Sei HACHISU

Institute for Optical Research, Tokyo University of Education

Sinzyuku-ku, Tokyo

(Received June 22, 1959)

Abstract

Electrophoresis in several organic solvents is studied on crystaline white lead treated with aerosel OT (sodium sulfonated dioctylsuccinate) or nitrocellulose. Aerosol treated pigment is positively charged in solvents in which it disperses, but not charged when it does not disperse. Nitrocellulose treated pigment, to the contrary, disperses in solvents which dissoluve nitrocellulose whether it is charged or not.

1. Introduction

It was described in the previous paper that crystalline basic lead carbonate flushed with nitrocellulose as well as with aerosol OT has particular dispersion characteristics for several organic liquids.

Some studies[1)2)3)] on the dispersion stability of inorganic pigments in oily media have been carried out. Kaelmans and Overbeek[3)] concluded that the dispersion of particles in a non-polar liquid is stabilized in two ways according to the size of the particles: for coarse particles by electric charge and for small particles by entropic effect (steric hindrance) of adsorbed layer. To be precise, in the case of large particles, the London-Van der Waals attractive force between the particles reaches so far away as compared to the thickness of adsorbed monomolecular layer (20 Å in case of surfactant) that the layer can no longer prevent the particles from agglomerating, and so the electric charge becomes nescessary for the stabilization of dispersion. But it is not so in the case of small particles ($\phi \fallingdotseq 100$ A) in which the London-Van der Waals force is weak; the particles are stabilized by the steric hindrance of the adsorbed monomolecular layers.

The pigment used in the present study consists of coarse particles (10 μ in diameter, about 700 Å in thickness). So the pigment, flushed with aerosol-OT, will

1) Machor & Van der Waals; J. Colloid Sci., 7, (1952) 535
2) Van der Minne & Hermanie; J. Colloid Sci, 7, (1952) 600; 8, (1953) 38
3) H. Koelmans, J. T. H. G. Overbeek; Discussion of Faraday Soc., 18, (1954) 52

disperse stably only when the particles have a certain amount of electric charge, but flushed with nitrocellulose, electric charge will not be necessary for dispersion because of the steric hindrance of high polymer molecules. In this aspect, the electrophoresis of the flushed pigments in several organic solvents was observed in corelation with dispersion stability.

Strict measurement of electrophoretic velocity is impossible with such coarse particles on account of their high sedimentation velocity. A simple boundary method was used in which the ascending velocity of the boundary in a virtical tube was measured. In this method, however, if the electric conductivity of dispersion medium is lower than 10^{-10} mho.,[2] the measurement becomes very tedious because of the leakage of current through the walls of apparatus.

Fortunately, since most of solvents used in this work had conductivity of the oder of 10^{-7}—10^{-8} mho., the experiments were carried out easily. In a few liquids of high resistance such as hydrocarbons, the pigments coagulated and no electrophoretic movement occurred at the field strengths applied in this experiment (5～20 volt/cm). ζ-potential is culculated from Helmholtz-Formula, but the calibration of electrophoretic velocity for which the effect of sedimentation of particles should be taken into consideration is not made. This value is not considered to be the real ζ-potential but a quantity corresponded to it and is expressed as $[\zeta]$ in this paper. As shown in the following, this quantity is in many cases closely related to the dispersion stability.

2. Experiment

One gram of the flushed pigment consisting of 60 % of the pigment and 40 % of dispersion medium as described in the previous paper was dropped into 30 cc of a solvent in which the dispersion was to be examined. The whole mixture containing 2 % of the pigment and 1 % of the initial medium (dichloromethane or butylacetate) was then shaken up in a stoppered glass cylinder.

The apparatus is shown in Fig. 1. A nickel electrode is fitted at each end of a glass tube, 25 cm in length and 12 mm in inner diameter. The distance between the electrodes is 20 cm.

The mixture was poured into this tube in horizontal setting, and 500 volt of direct current potential was applied.

As the pigment particles had electric charge, they were forced to move leaving in a few minutes a transparent space near one of the electrodes as shown in Fig. 2 which determined the polarity of the particles. The tube was then made vertical with the transparent end down. After all the particles were well settled at the bottom, the electric field was again applied at 100～200 volt.

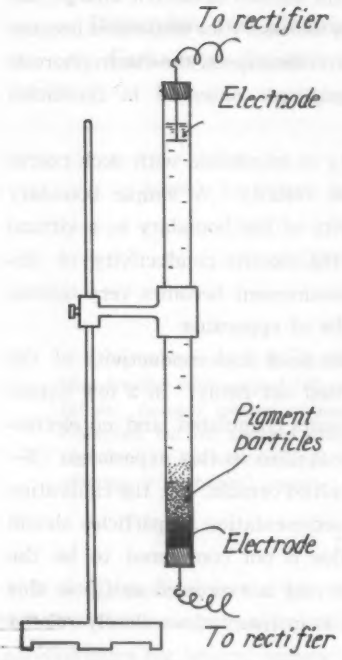

Fig. 1

Sedimented pigment layer swelled gradually and diffused upward as shown in Fig. 3. The boundary between the rising particles and clear liquid was well difined and steadily ascended, while the lower boundary between rising and remaining particles disappeared in time. The distance of this rising uper boundary measured from its initial position was regarded as the electrophoretic distance and plotted against time from which the electrophoretic velocities were obtained. Observation were made at 18°~20°C. In Fig. 4, the electrophoretic distancies of aerosol flushed and nitrocellulose flushed pigment are plotted.

3. Summary of the Results

General feature of the experiments was as follows.

1. Pigment dispersed well and regular shift of boundary was observed.

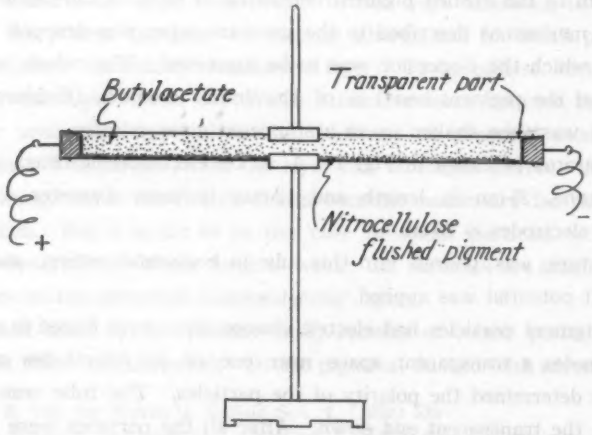

Fig. 2

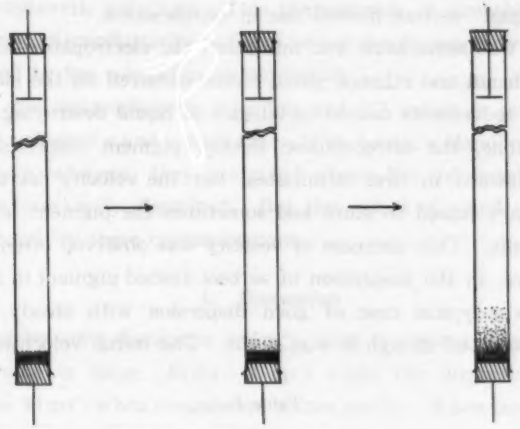

Fig. 3

Example: nitrocellulose flushed pigment in butylacetate and ethylacetate, electric charge of particles was negative: aerosol flushed one in dichloromethane and butylalcohol, electric charge was positive.

2. Pigment dispersed well but no migration was observed.

Example: nitrocellulose flushed pigment in pyridine and methylcellosolve.

3. Pigment coagulated and no migration was observed.

Example: aerosol flushed pigment in hydrocarbons, carbontetrachloride, butylacetate.

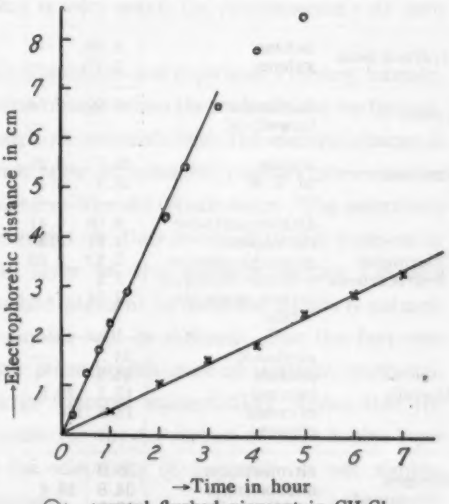

Fig. 4

In this case, on raising the voltage to 500 volt/20 cm, no steady migration but turbulent movement or streak formation[3] occured.

4. Pigment dispersed partly and migration was observed in the dispersing part, the other part coagulated and showed no migration. In this case [ζ] was small.

Example: aerosol flushed one in nitrobenzene.

5. Electrolysis was remarkable and influenced the electrophoresis.
   (a) In methanol and ethanol, small foams occurred on the electrode and their ascending movements caused turbulence of liquid destroying the boundary.
   (b) In acetone, the nitrocellulose flushed pigment dispersed and migrated steadily upward in first 30 minutes, but the velocity decreased and finally the boundary ceased to move and sometimes the pigment fell down or stuck to the walls. This decrease of velocity was observed often in other cases, for instance, in the suspension of aerosol flushed pigment in dichloromethane which was a typical case of good dispersion with steady migration, this decrease occurred though it was slight. The initial velocities were taken as

Table 1.

Solvents		ε	$\eta\times10^3$	Nitrocell. Flushed Pigment			Aerosol OT Flushed Pigment		
				dis	$v\times10^5$	$[\zeta]\times10^3$	dis	$v\times10^5$	$[\zeta]\times10^3$
Hydrocarbons	hexane	1.89	—	×	0	0	×	0	0
	xylene	2.77	—	×	0	0	△	0	0
Esters	butylacetate	5.01	7.04	○	2.6	−42	△	0	0
	linseed oil	—	—	×	0	0	×	0	0
Ketones	aceton	20.7	3.31	○	15	−28	△	0	0
	M. E. K.	18.4	4.2	○	23	−60	△	0	0
Chlorinated hydrocarbons	dichloromethane	9.08	4.41	×	0	0	○	12	+66
	chloroform	4.81	5.63	×	0	0	○	2.8	+37
	monochlorobenze	5.53	8.03	△	0	0	□	1.2	+19
	o-dichlorobenzene	7.5	—	×	0	0	□	—	—
	carbon tetrachloride	2.24	—	×	0	0	×	0	0
Alcohols	methanol	33	—	○	0	0	×	0	0
	ethanol	24.3	—	○	0	0	×	0	0
	butanol	17.1	29.5	×	0	0	○	2.4	+47
	m-cresol	11.8	184	×	0	0	○	0.26	+47
	glycerol	—	—	×	0	0	×		
Nitrogen compounds	nitromethane	35.9	—	○	6.2	—	×	0	0
	nitrobenzene	34.8	19.8	○	1.1	−8	□	3.1	+20
	pyridine	12.3	8.77	○	0	0	□	3,1	+25
Others	ether	—	—	△	0	0	△	0	0
	ether+ethanol	—	—	○	0	0	△	0	0
	diacetone alcohol	—	—	○	0	0	△	0	0
	ethylenglycol monomethyl ether	—	—	○	0	0	△	0	0

dis: dispersion character
ε: electric susceptibility
v: electrophoretic velocity (cm/sec volt/cm)
η: viscosity
$[\zeta]$: $\frac{4\pi\eta v}{\varepsilon}$ volt

the electrophoretic velocities. This phenomenon is probably resulted from the decrease of conductivity of liquid owing to inhomogenity of ion concentration caused by ion migration in the liquid.

In Table 1. the electrophoretic velocities and [ζ]-values in several liquids are tabulated. The values of ε and η were taken from Lange's Handbook of Chemistry. The solvents were not pure; they contained about 1 % of butylacetate or dichloromethane as previously described. But the values of ε and η would not have been much affected by these contaminations.

4. Discussion

The relation between dispersion and [ζ]-value is obvious in aerosol-OT flushed pigment. [ζ]-value is large (40 mv—60 mv) when the dispersion is stable; it ts small (less than 30 mv) when coagulation occurs partly. When thoroughly coagulated [ζ] is zero.

In nitrocellulose flushed pigment, this relation does not exist, and even in the case of complete dispersion, the [ζ]-value is very small (in nitrobenzene) or zero (in methylcellosolve).

These results are in accordance with Koemanns and Overbeek's theory, namely, the coarse particles are stabilized by electric charge when they adsorb the surfactant, but when they adsorb high polymer, such as nitrocellulose, the electric charge is not necessary for dispersion, for the thick layer of adsorbed polymer prevents the particles from coming into the range of London-Van der Waals force. The selectivity of dispersion of aerosol-OT flushed pigment is thus ascribed to the easiness or difficulty of forming of electric double layer on the pigment surface. In this viewpoint, the coagulation of aerosol flushed pigment in nonpolar liquids is natural, for the ion-formation in these nonpolar liquids will be difficult. But the fact that the pigment does not disperse in high polar liquids such as acetone, methanol, methylethylketone which have very large electric susceptivility shows that the polarity of the liquids is not the only cause for the formation of ionic double layer on the particles. Exact explanation of the selectivity of dispersion is not simple, for which detailed study would be necessary.

In the case of nitrocellulose flushed pigment, it is apparent that adsorbed polymer molecules act as protective colloid.

Solvent Effect on Spectrum and Association Constant for Phenol-Dioxane Complex Formation Extrapolated to Gaseous State

Yoshiki SATO
Institute for Optical Research, Tokyo University of Education
Sinzyuku-ku, Tokyo

(Received July 21, 1959)

Abstract

Association constant in hydrogen bonding between phenol and dioxane is determined in various solvents by using infrared absorption spectrum. On the basis of the linear relationship found between the logarithm of the association constant and the relative frequency shift of hydroxyl stretching mode of phenol, solute-solvent interaction is discussed.

1. Introduction

The influence of solvent on infrared absorption spectrum has been studied by many investigators[1], and the dielectric constant of the solvent is being considered responsible for causing the spectral shift as stated in Kirkwood-Bauer-Magat theory[2-4]. Of late, Bellamy et al.[5-7] on the other hand suggested that local association effect is predominant rather than dielectric constant in producing the spectral shift. The influence of solvent on association constant in the process of hydrogen bond formation is determined by that on the free energy change in the said process which, as will be discussed later in full, seems to be effected by solvation energy of solvent molecules lying within a small solid angle around the line joining two electronegative atoms in the hydrogen bond system. The solvation energy of those particular solvent molecules is regarded as closely related to the frequency shift of the functional group partaking in hydrogen bonding. Therefore, elucidation of the influence of solvent on association constant will throw light upon the nature of the frequency shift caused by the solvent. For that reason, the association constant in hydrogen bonding between phenol and dioxane was determined in various solvents by using the spectral absorption method and investigated in relation to the frequency shift.

1) M.-L. Josien and N. Fuson: J. Chem. Phys. **22** (1954) 1169, and cited papers in there.
2) W. West and R.T. Edwards: J. Chem. Phys. **5** (1937) 14.
3) W. West: J. Chem. Phys. **7** (1939) 795.
4) E. Bauer and M. Magat: J. Phys. Radium **9** (1938) 319.
5) L.J. Bellamy, H.E. Hallam and R.L. Williams: Trans. Faraday Soc. **54** (1958) 1120.
6) L.J. Bellamy and R.L. Williams: Trans. Faraday Soc. **55** (1959) 14.
7) L.J. Bellamy and H.E. Hallam: Trans. Faraday Soc. **55** (1959) 220.

2. Experimental and Results

The association constant, K, for the type of the system described above is

$$K=C_{AB}/(C_A-C_{AB})(C_B-C_{AB}) \tag{1}$$

where C_{AB} is concentration in mole per litre of hydrogen bonded complex, C_A that of phenol, and C_B that of dioxane. C_{AB} varies with C_B. Hence, for a given C_A, it is always possible to determine C_B to satisfy the relation

$$C_{AB}/(C_A-C_{AB})=1/n\,, \tag{2}$$

in which n is larger than 1. Eq. (2) leads directly to

$$C_{AB}=C_A/(n+1) \tag{3}$$

and further to

$$C_A/(C_A-C_{AB})=(n+1)/n\,. \tag{4}$$

Substituting Eqs. (2) and (3) into Eq. (1), K can be rewritten as

$$K=1/n(C_B-C_A/(n+1))\,. \tag{5}$$

In evaluating K from Eq. (5), the following two ways are contemplated by assuming the validity of the Lambert-Beer law for phenol. (a) Optical densities D and D' of O-H stretching stretching vibration band of unassociated phenol measured at $C_B=0$ and $C_B\neq 0$ give

$$C_A=D/\varepsilon_A 1$$

and

$$C_A-C_{AB}=D'/\varepsilon_A 1\,,$$

where ε_A is the maximum molar absorption coefficient and 1 the cell thickness. Eq. (4) then becomes

$$C_A/(C_A-C_{AB})=D/D'=(n+1)/n\,.$$

This gives n with which K can readily be determined from Eq. (5). Several values of K thus obtained for different values of n are averaged. (b) A smooth curve of optical density of the unassociated band of phenol versus concentration C_B of dioxane is drawn. C_B that satisfies Eq. (4) for a given n is then found with which K can be calculated by Eq. (5). The most probable value of K is obtained by averaging as in the case (a). The relation between the concentration of phenol and the optical density of the first overtone band of the O-H stretching vibration of phenol obtained in chloroethylene solution is shown in Fig. 1 which follows the Lambert-Beer law at least in the range of concentrations used. Fig. 2 shows the

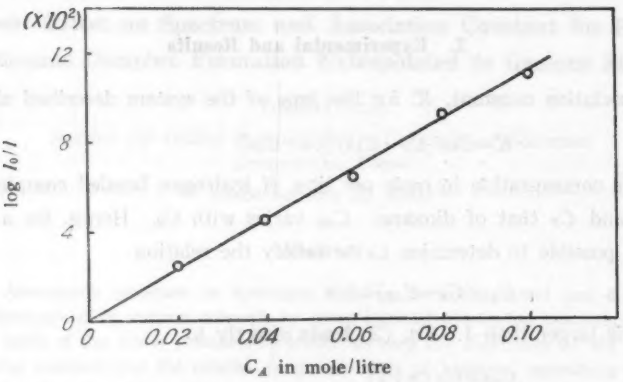

Fig. 1. Optical density of O–H stretching band of phenol versus phenol concentration in mole/litre. Solvent: tetrachloroethyne. Cell thickness 2 cm.

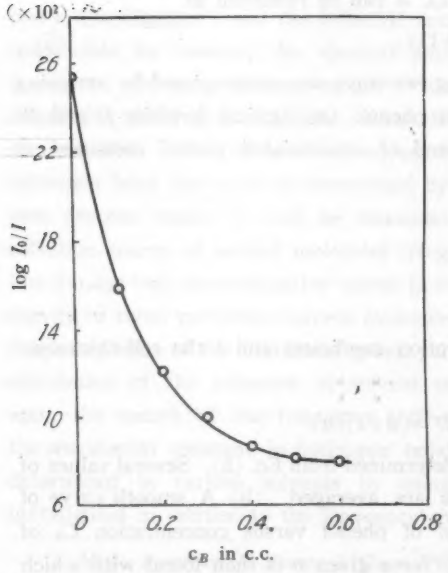

Fig. 2. Optical density of O–H stretching band of unassociated phenol versus volume concentration of dioxane. Solvent: benzene. Cell thickness 2 cm.

optical density plotted against the volume of dioxane added in carbon tetrachloride solution. The volume was later converted to molar concentration by measuring its specific gravity. Fig. 3 is for the case in which benzene was used as solvent, the curve I corresponding to the maximum absorption and the curve II to absorption at a wavelength shorter than that of the former. Values of K estimated from these two curves by applying the second method described above are in considerably good agreement with each other within experimental error. Values of the association constant thus determined are listed in Table 1 together with the names of solvent. All of the samples used were reagent grade, some of which were redistilled before being used. Spectral data were obtained with a near infrared grating spectrometer already reported. Cell thickness was 2 cm.

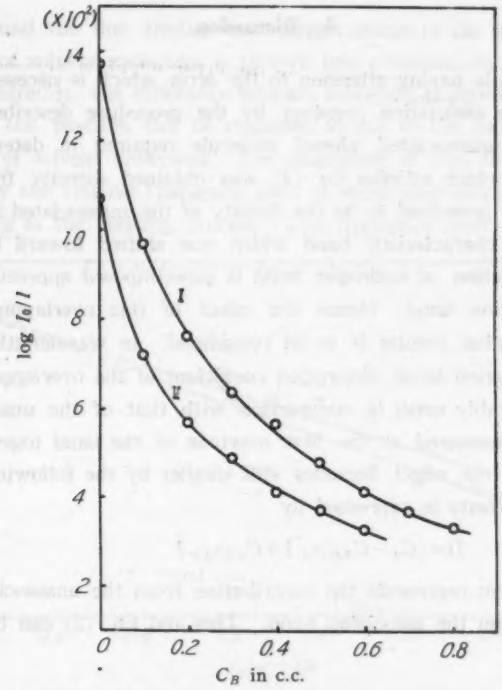

Fig. 3. Optical densities at two different wavelengths of O-H stretching band of unassociated phenol versus volume concentration of dioxane. Solvent: benzene. Cell thickness 2 cm.

Table 1. Association constants for hydrogen bond formation between phenol and dioxane at 17°C and relative frequency shifs of functional groups of phenol and pyrrole in different solvents.

Solvent	K	log K	$(\Delta\nu/\nu)\times10^2$ ν (NH)	$(\Delta\nu/\nu)\times10^2$ 3ν (OH)
Carbon tetrachloride	11.2	1.05	0.94	1.17
m-Xylene	3.4	0.53	2.41	
Benzene	4.0	0.60	2.04	2.65
Tetrachloroethylene	8.1	0.83		1.21
Toluene	3.7	0.57	2.32	2.99
Carbon disulfide	9.6	0.98	1.39	1.60
Dichloroethane	4.5	0.65	1.84	
sym-Tetrachloroethane	6.8	0.83	1.56	

3. Discussion

It is worth while paying attention to the error which is necessarily introduced in determining the association constant by the procedure described above. The concentration of unassociated phenol molecule required in determining experimentally n or C_B which satisfies Eq. (4) was obtained directly from the optical density which was presumed to be the density of the unassociated absorption band. The wing of the characteristic band which was shifted toward lower frequency side by the formation of hydrogen bond is superimposed appreciably on the unassociated absorption band. Hence the effect of this overlapping from which the error in question results is to be considered. In wavelength regions of the unassociated absorption band, absorption coefficient of the overlapped band would usually be considerably small in comparison with that of the unassociated band, especially, when measured at the first overtone of the band together with small C_B. Furthermore, the effect becomes still smaller by the following reason. The observed optical density is expressed by

$$D=(C_A-C_{AB})\varepsilon_A 1+C_{AB}\varepsilon_{AB} 1$$

where the first term represents the contribution from the unassociated band, and the second that from the associated band. This and Eq. (2) can be combined to give

$$D=(C_A-C_{AB})\left(\varepsilon_A+\frac{\varepsilon_{AB}}{n}\right) 1 .$$

The effect of the overlapping of the associated band can be reduced to one nth becoming negligibly small for appropriate values of n.

Next, the association constant listed in Table 1 is discussed. The effect of solvent on the association constant is nothing but that on the difference between solvation energies in initial and final states of the equilibrium reaction. In the initial state in which phenol and dioxane molecules are beyond the range of mutual interaction, every one of these molecules is surrounded by and bound to solvent molecules. In the final state in which phenol and dioxane molecules are hydrogen-bonded, change in orientation of those solvent molecules that surrounded the solute molecules is considered not so much as to cause appreciable effect on the outcome, for, although there is to some extent reorientation of solvent molecules to respond to the change in distribution of charge on solute molecules as the result of the hydrogen bond being formed, this change is not significant as infered from observation of electronic spectra or dipole moment. However, we see a great change in the contribution to solvation energy by solvent molecules lying within a small

solid angle around the line joining two oxygen atoms in the hydrogen bond, for the orientation of solvent molecules is thrown into confusion by the steric growth of the bond. Therefore, the difference between solvation energies in the initial and final states of the reaction can be regarded as due to the contribution by those limited number of solvent molecules. The magnitude of this difference may likely be estimated by the relative frequency shift of stretching vibrations of functional groups partaking in the bonding process. The frequency shift caused by solvent

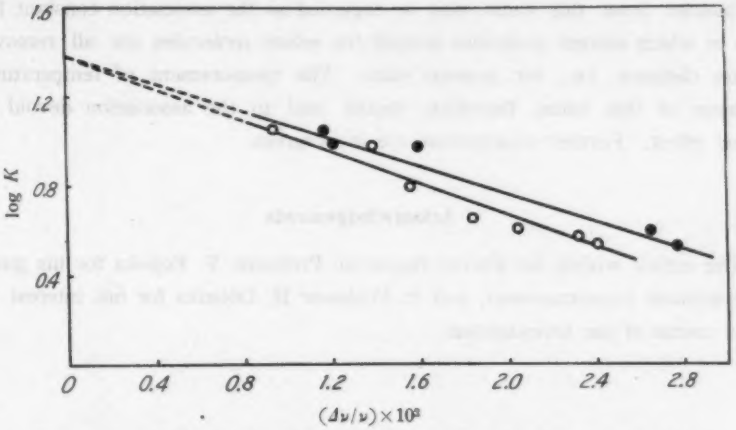

Fig. 4. Logarithm of association constant versus relative frequency shift, ● phenol, and ○ pyrrole.

is closely related to the change in free energy accompanying the solvation under consideration. Then, plotting the logarithm of the association constant, which is also closely connected to the free energy change accompanying the hydrogen bond formation, against the solvent shift $(\Delta\nu/\nu)$ of phenol by using the data of Luttke et al.[8,9] Fig. 4 is obtained. The linear relation between the variables is clearly seen on the plot, and is also for solvent shifts of pyrrole[1] and hydrogen chloride[5,10]. Such a fact seems to give, in reference to the above, a direct evidence for local association effect which was suggested by Bellamy et al. as the dominant factor in producing frequency shifts and was expected for aromatics and olefins from specific interaction between their π-electron clouds and the OH group.

Furthermore, as the free energy change accompanying the bond formation in its final state seems to be influenced only by the energy of mutual interaction between the hydroxyl group of phenol and the surrounding solvent molecules,

8) W. Luttke and R. Mecke: Z. Electrochem. **53** (1949) 241.
9) R. Mecke: Disc. Faraday Soc. **9** (1950) 161.
10) M.-L. Josien and G. Sourisseau: Bull. Soc. Chim. (1955) 178.

assumption may be made that the influence of solvent on bond formation is small which is in agreement with what Fuson et al.[11] found in the bond formation of NH-containing compounds. Besides, the interaction force acting between non-bonding electrons of dioxane and solvent molecules does not seem to be strongly directional, and as shown in the figure, it is worthy of note that values of $\log K$ obtained by extrapolating each of the three straight lines to $(\Delta\nu/\nu)=0$ are in good agreement with one another, their average values being about 1.4. The value of K obtained from this value may be regarded as the association constant for the state in which solvent molecules around the solute molecules are all removed to infinite distance, i.e., for gaseous state. The measurement of temperature dependence of this value, therefore, should lead to the association devoid of the solvent effect. Further experiments are in progress.

Acknowledgements

The author wishes his sincere thanks to Professor Y. Fujioka for his guidance and continued encouragement, and to Professor H. Ootsuka for his interest taken in the course of the investigation.

11) N. Fuson, M.-L. Josien, R.L. Powell and E. Utterback: J. Chem. Phys. **20** (1952) 145.

CONTENTS

moved to Back of Vol. 7